Volume 48 | Number 24 | 28 June 2019 | Pages 8505–9006

Dalton Transactions

An international journal of inorganic chemistry

rsc.li/dalton

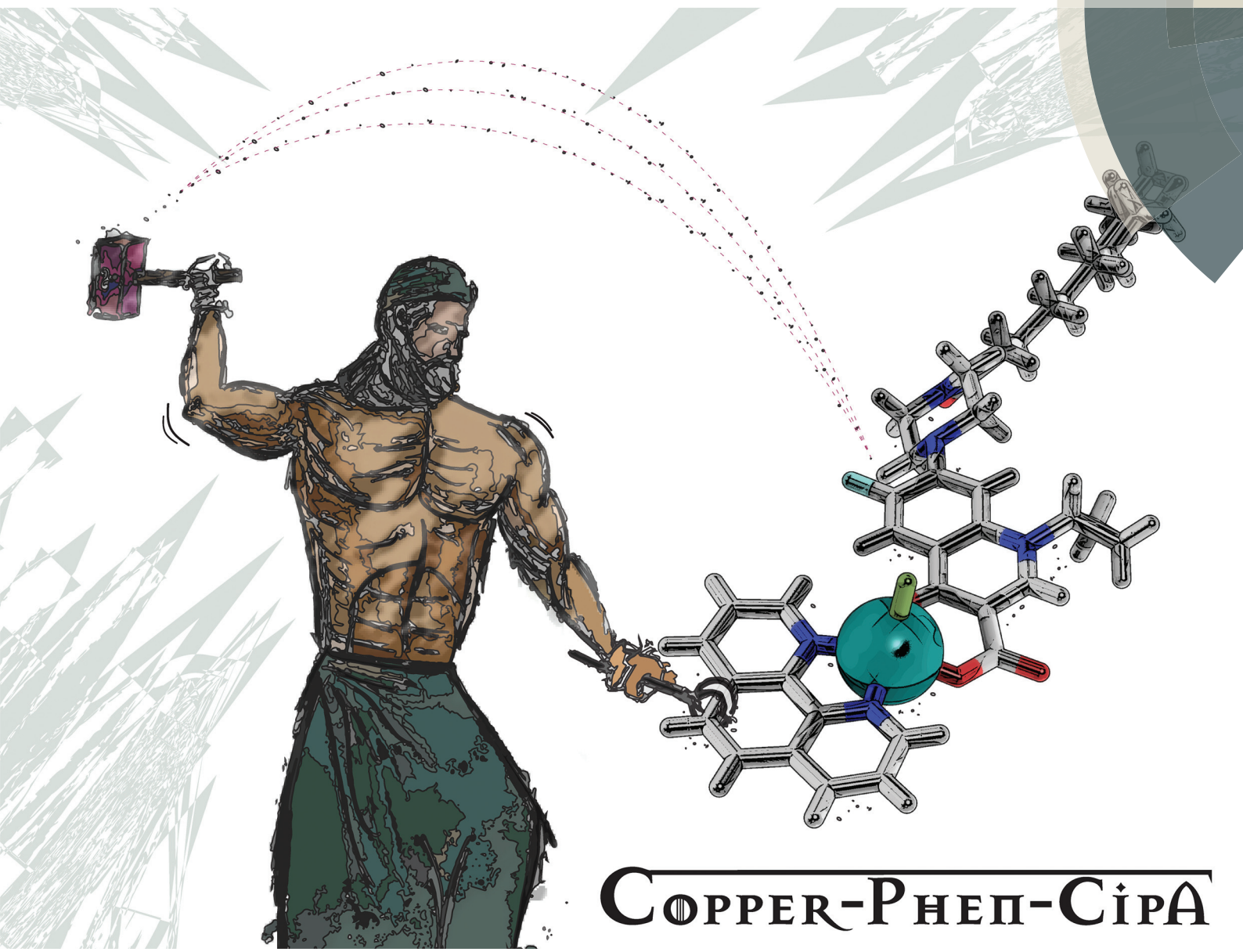

ISSN 1477-9226

ROYAL SOCIETY OF CHEMISTRY | Celebrating IYPT 2019

PAPER

Andrew Kellett, Celine J. Marmion *et al.*

A new class of prophylactic metallo-antibiotic possessing potent anti-cancer and anti-microbial properties

Dalton Transactions

PAPER

View Article Online
View Journal | View Issue

Cite this: *Dalton Trans.*, 2019, **48**, 8578

A new class of prophylactic metallo-antibiotic possessing potent anti-cancer and anti-microbial properties†

Ziga Ude,[a] Kevin Kavanagh,[b] Brendan Twamley,[c] Milan Pour,[d] Nicholas Gathergood,[e] Andrew Kellett *[f] and Celine J. Marmion *[a]

Immunocompromised cancer patients are often at high risk of developing infections. Standard infection control measures are required to prevent the onset of infection but, under some circumstances, antimicrobial prophylaxis is necessary. We have developed a family of innovative metallo-antibiotics of general formula [Cu(N,N)(CipA)Cl] where N,N represents a phenanthrene ligand and CipA stands for a derivative of the clinically used fluoroquinolone antibiotic ciprofloxacin. The X-ray crystal structure of one member from this family, [Cu(phen)(CipA)Cl] (where phen is 1,10-phenanthroline), is also reported. These complexes combine into one drug entity a Cu-N,N-framework with DNA binding and DNA oxidant properties and an antibiotic derivative with known anti-proliferative and anti-microbial activities. The complexes were all found to exhibit excellent DNA recognition with binding affinity of lead agents in the order of $\sim 10^7$ M(bp)$^{-1}$. Biophysical studies involving calf thymus DNA indicate the complexes intercalate or semi-intercalate DNA *via* the minor groove. All complexes exhibited excellent nuclease activity with DNA strand scission being mediated predominantly *via* superoxide and hydroxyl radicals. The complexes were found to have promising anti-proliferative effects against a human breast adenocarcinoma cell line (MCF-7) and a human prostate carcinoma cell line (DU145) with low micromolar and, in some cases, nanomolar cytotoxicities observed. Selective targeting of Gram positive bacteria was also identified by this complex class with one lead compound having an order of magnitude greater potency against Methicillin-resistant *S. aureus* (MRSA) as compared to the CipA ligand. Importantly, from a clinical stand point, these complexes were also found to be well tolerated in an *in vivo Galleria mellonella* larvae model, which has both functional and structural similarities to that of the innate immune system of mammals.

Received 18th January 2019,
Accepted 26th March 2019

DOI: 10.1039/c9dt00250b

rsc.li/dalton

1. Introduction

DNA represents an important target for many cancer therapeutics. For example, platinum drugs, which are amongst the most widely utilised therapeutics in cancer treatment regimens, irreversibly bind to DNA nucleobases.[1] This results in the formation of DNA lesions, which ultimately leads to tumour cell apoptosis or programmed cell death.[1] Despite their enormous clinical success, many platinum drugs have shortcomings, not least dose-limiting toxic side effects and acquired or intrinsic drug resistance.[1,2] A number of research strategies are being actively pursued in an attempt to overcome these drawbacks. These include the exploitation of nanotechnologies, which can selectively deliver platinum(II) payloads to tumours.[2] An alternative strategy is to develop non-platinum based drugs with a mechanism of action and toxicity profile different to classical platinum therapies. In this regard, copper complexes are being actively explored on the assumption that complexes incorporating endogenous metal ions

[a]*Centre for Synthesis and Chemical Biology, Department of Chemistry, Royal College of Surgeons in Ireland, 123 St. Stephen's Green, Dublin 2, Ireland. E-mail: cmarmion@rcsi.ie*
[b]*Department of Biology, Maynooth University, Maynooth, Co. Kildare, Ireland*
[c]*School of Chemistry, Trinity College Dublin, University of Dublin College Green, Dublin 2, Ireland*
[d]*Department of Organic and Bioorganic Chemistry, Faculty of Pharmacy, Charles University, 500 05 Hradec Kralove, Czech Republic*
[e]*ERA Chair of Green Chemistry, Division of Chemistry, Department of Chemistry and Biotechnology, School of Science, Tallinn University of Technology, Akadeemia tee 15, 12618 Tallinn, Estonia*
[f]*School of Chemical Sciences and the National Institute for Cellular Biotechnology, Dublin City University, Dublin 9, Ireland. E-mail: andrew.kellett@dcu.ie*

†Electronic supplementary information (ESI) available: Miscellaneous information and X-ray crystallographic data of Cu(phen)(CipA)Cl. CCDC 1586315. For ESI and crystallographic data in CIF or other electronic format see DOI: 10.1039/c9dt00250b

such as copper(II) may be less toxic to normal cells and may thus give rise to less toxic side effects.[3] Copper complexes may also have a mechanism of action and therefore cytotoxicity profile different to platinum-based drugs and may thus also potentially evade the chemoresistance related to recurrent platinum drug treatments. It is also noteworthy that known platinum reserves will be depleted within *ca*. 50 years.[4] Cancer therapeutics based on relatively more abundant metals (*e.g.* copper) are therefore also of great interest.

The majority of the copper(II) complexes reported to-date as potential anti-cancer agents, target DNA. Four modes of DNA binding have been reported; (i) electrostatic, (ii) groove binding, (iii) intercalation, and/or (iv) direct binding to DNA nucleobases.[3b] Copper complexes can also cleave DNA strands either *via* hydrolysis of the phosphodiester backbone or by an oxidative mechanism whereby H-atom abstraction from the deoxyribose ring of DNA occurs.[5] Such oxidative DNA cleavage is predominantly mediated *via* the formation of reactive oxygen species (ROS) generated either by a redox- or photo-induced process[3a,b] although there are some examples of copper complexes acting as self-activating DNA nuclease agents.[6] Sigman *et al.* discovered the artificial chemical nuclease properties of copper(I) bis-1,10-phenanthroline systems. The Cu-bis-phenanthroline complex, $[Cu(phen)_2]^{2+}$ (where phen is 1,10-phenathroline) Fig. 1 (**1**), for example, is capable of inducing oxidative DNA damage in the presence of a reductant (and oxidant, *e.g.* O_2) through free radical oxidation of deoxyribose.[7] This complex, however, binds without specificity, to a number of different targets including not only double stranded DNA but also protein biomolecules.[3c] In an effort to enhance DNA binding and intercalation, Kellett *et al.* rationally designed and developed a series of cationic phenazine functionalised copper(II)-phen complexes of formula [Cu(DPQ)(phen)] $(NO_3)_2$ (**2**), [Cu(DPPZ)(phen)]$(NO_3)_2$ (**3**), and [Cu(DPPN)(phen)] $(NO_3)_2$ (**4**) (where DPQ = dipyridoquinoxaline, DPPZ = dipyridophenazine, and DPPN = benzo[*i*]dipyridophenazine), Fig. 1.[8] By systematically extending the phenazine ligand from phen to DPQ to DPPZ, the resulting complexes could not only influence DNA recognition but also induce oxidative DNA degradation. In fact, the calf thymus DNA (ctDNA) binding constants ($\sim 10^7$ $M(bp)^{-1}$) for these complexes are amongst the highest currently reported for copper(II)-phenanthrene systems. The complexes were also highly cytotoxic toward a cisplatin-resistant ovarian cancer line, comparable to that of the clinical oxidative DNA-damaging drug doxorubicin (Adriamycin).[8]

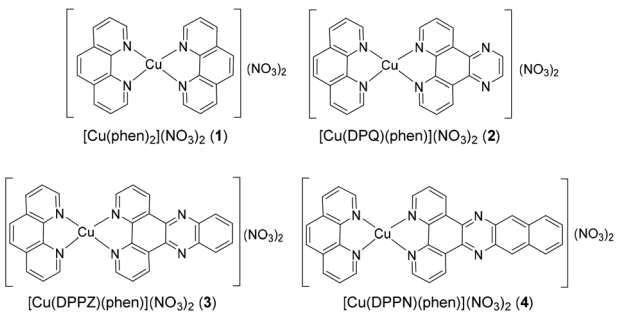

Fig. 1 Molecular structures of ternary copper(II) complexes incorporating 1,10-phenanthroline (phen) and phenanthrene (DPQ; DPPZ; or DPPN) ligands.

Inspired by the potential inherent in the aforementioned Cu-phenazine derivatives (**1–4**) along with more recent advances in this field,[9] we sought to exploit this Cu-phenazine framework as a platform in which to add additional therapeutic moieties. We specifically sought to introduce an antimicrobial agent on the basis that cancer patients, particularly those who sustain neutropenia (where the white blood cell count is lower than normal) during the course of their disease, are often highly predisposed to infections.[10] Therapy-related myelosuppression and immune defects inherent in the cancer disease process are also notable risk factors for infection.[11] The use of central venous catheters (CVCs) for the administration of chemotherapeutic agents can also pose significant risk. Bacteraemia rates in cancer patients, resulting from central line associated bloodstream infections (CLABSIs), range from 11–38%.[12] Mortality rates of 9.6%, arising from CLABSI, have been reported in paediatric oncology patients.[13] Prophylactic anti-microbial therapies may be an option in targeted cancer patients or cancer populations being treated at institutions in which high rates of CLABSIs, despite infection control, are observed.[12] In addition, peri/post-operative antibiotic prophylaxis (POABP) has become standard practice in an attempt to prevent surgical site infections in head and neck cancer patients following microvascular reconstruction.[14]

Quinolones, and especially fluoroquinolones, are widely utilised in human medicine to treat both Gram-negative and Gram-positive bacterial infections.[15] Topoisomerases—enzymes that mediate the topical changes in DNA during a range of processes are considered to be one of the main targets of quinolones.[15] Several copper(II) complexes incorporating fluoroquinolones have been reported including a moxifloxacin (Moxi) derivative $[Cu(Moxi)_2(H_2O)_2]$,[16] and a Hpr-norfloxacin (Hpr-norf) derivative [Cu(Hpr-norf)(bpy)Cl].[17] While these complexes exhibited anticancer activity, to the best to our knowledge, their anti-microbial properties were not investigated. Ciprofloxacin (Cip), Fig. 2 (**5**), a member of the fluoroquinolone family, is particularly important since it is classified as an essential medicine by the World Health Organization.[18] A copper(II) complex incorporating two Cip ligands, $[Cu(Cip)_2(ClO_4)_2]$, has been reported.[19] It exhibited higher potency as an anti-bacterial against two strains of the Gram positive bacterium *Staphylococcus aureus* (*S. aureus*) when compared to Cip itself. Interestingly, and in contrast to Cip alone, the complex was found to be more damaging against stationary phase bacteria, a property which may be attractive for the treatment of chronic or device-related infections (such as catheter infections) which involve slowly metabolising bacteria in biofilm mode. The X-ray crystal structure of [Cu(phen)(Cip)Cl] Cl has also been reported but its anti-cancer and anti-microbial properties were not evaluated.[20]

While the anti-microbial properties of Cip are well known, Azema *et al.* developed a library of Cip derivatives with a view

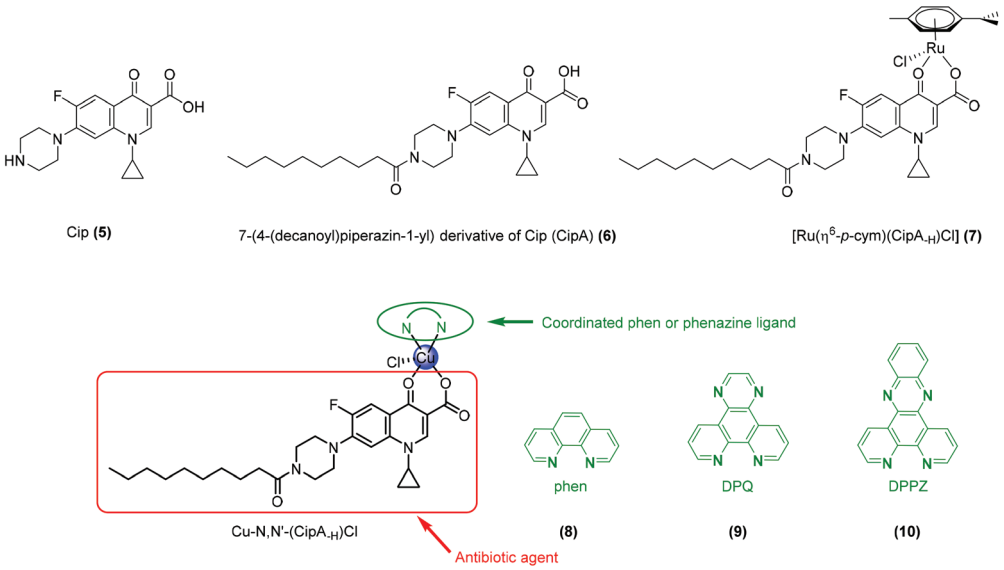

Fig. 2 Chemical structures of Cip (**5**), CipA (**6**) and [Ru(η^6-p-cym)(CipA$_{-H}$)Cl] (**7**) and of the Cu-N,N-(CipA$_{-H}$)Cl complexes (**8–10**).

to assessing their anti-cancer potential.[21] Of these, the 7-(4-(decanoyl)piperazin-1-yl) derivative CipA, Fig. 2 (**6**), was particularly cytotoxic (in the low μM range) against a range of tumour cell lines, indeed much more so than Cip itself. This derivative was also non-toxic in an *in vivo* xenograft mouse model. To further expand this class of compounds, we recently reported a ruthenium(II)–arene complex incorporating this Cip derivative, Fig. 2 (**7**). This complex possessed potent *in vitro* cytotoxicity against a small range of tumour cell lines but only exhibited moderate anti-microbial activity.[22]

Given that copper(II) complexes have demonstrated significant potential as anti-microbial agents,[23] we sought to combine into one drug molecule, the Cu-phenazine framework with the Cip derivative CipA (**6**) with the expectation of generating a multi-modal therapeutic possessing both potent cytotoxicity and anti-microbial properties, Fig. 2.

In this contribution, we report the synthesis and biological evaluation of the first examples of a family of [Cu(N,N)(CipA)Cl] derivatives, herein referred to as Cu-N,N-CipA, in which N,N is phen (**8**), DPQ (**9**) or DPPZ (**10**). Through structure–activity relationship studies, we sought to ascertain whether we could modulate or enhance the anti-microbial activity of this Cip derivative *via* complexation to a Cu-phenazine framework whilst retaining or enhancing its cytotoxic potential. We specifically investigated the ability of our Cu-N,N-CipA complexes to induce DNA damage *via* intercalation and/or ROS-mediated DNA cleavage. Their ability to inhibit topoisomerase I was also investigated given that these enzymes are one of the main targets of fluoroquinolones. Cytotoxicities of **8–10** were assessed against a human breast adenocarcinoma cell line (MCF-7) and a human prostate carcinoma cell line (DU145). The complexes, **8–10**, were also screened for anti-microbial and anti-fungal activity. Furthermore, a preliminary *in vivo* study was undertaken using a *Galleria mellonella* (*G. mellonella*) larvae model to assess their toxicity profile. A summary of these findings is presented herein.

2. Results and discussion

2.1. Synthesis and characterisation of the Cu-N,N-CipA complexes

The ligands phendione, DPQ and DPPZ[8] and CipA[21] were synthesised according to previously published methods. Schiff-base condensation of phendione with either ethylenediamine or 1,2-phenylenediamine afforded the phenazine ligands DPQ and DPPZ respectively. Treatment of an aqueous solution of $CuCl_2{\cdot}2H_2O$ with one molar equivalent of phen, DPQ or DPPZ in hot ethanol, followed by the addition of one molar equivalent of a basic methanolic solution of CipA, afforded the complexes as green solids in excellent purity and good yield. Turquoise crystals of [Cu(phen)(CipA$_{-H}$)Cl], suitable for X-ray structure determination, were isolated. The asymmetric unit consists of a [Cu(phen)(CipA$_{-H}$)Cl] unit and one water and one methanol molecule, Fig. 3. The Cu^{2+} ion is coordinated by two CipA O atoms and two phen N atoms in the equatorial plane, and by a Cl ion in the axial position. It adopts a slightly distorted square pyramidal geometry, with an O15–Cu–O20 angle of 93.18(15)° and a N1–Cu–N12 angle of 81.11(17)°. All bond lengths and angles are in agreement with literature values.[24] For example, distances between Cu^{2+} and the CipA O's are 1.909(4) Å and 1.944(3) Å, respectively, consistent with literature reports.[24] The Cu1–Cl1 bond length is 2.4757(13) Å, again within the expected range. Metal-to-ligand distances are also similar to those found in related compounds where Cu^{2+} ion is coordinated to cinoxacin, nalidixic acid,[25] and to Cip.[20] The complex is almost planar, with the exception of the piperazine ring, which has a slightly affected chair conformation due to

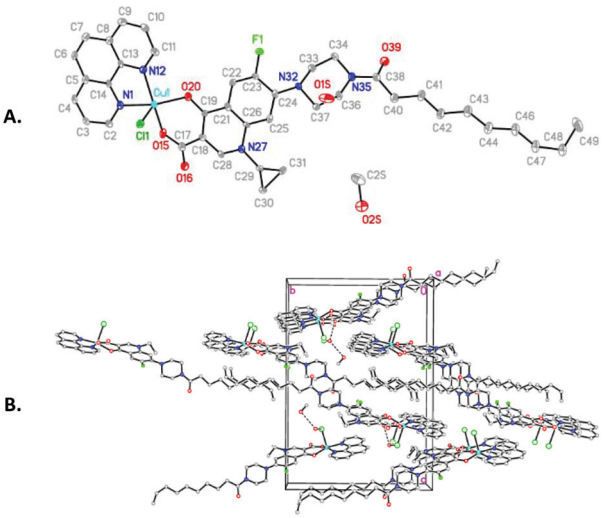

Fig. 3 (A) Molecular structure of [Cu(phen)(CipA$_{-H}$)Cl]·1H$_2$O·1CH$_3$OH with atomic displacement parameters shown at 50% probability. Only one conformation of the disordered chain is shown and hydrogen atoms omitted for clarity. (B) Packing diagram of [Cu(phen)(CipA$_{-H}$)Cl] (major moiety) viewed down the c-axis. Hydrogen atoms omitted for clarity.

the presence of the aliphatic chain, and the cyclopropyl ring, which makes a dihedral angle of 38.63(1)° with the Cu(phen)(CipA$_H$) plane. [Cu(phen)(CipA$_H$)Cl] co-crystallised with a mixture of water and methanol (one molecule of each). The packing diagram of [Cu(phen)(CipA$_H$)Cl] suggests molecules of [Cu(phen)(CipA$_H$)Cl] in each cell unit being connected to each other *via* hydrogen bonds, where molecules of water form strong hydrogen bonds with the carbonyl O's of CipA (d(O16–O$_{water}$) of 2.754(6) Å and the Cl's (d(Cl1–O$_{water}$) of 3.134(4) Å.

ESI mass spectra of all complexes (**8–10**) (ESI – SI†) revealed m/z peaks corresponding to [Cu(N,N)(CipA$_H$)]$^+$ as expected. IR spectroscopy also confirmed each compound to contain vibrational peaks characteristic of coordinated aromatic imines and carboxylate ligands and consistent with complexation to the copper(II) ion *via* the pyridone O and deprotonated carboxylate O[26] with X-ray crystallographic analysis of [Cu(phen)(CipA$_H$)Cl] confirming this mode of binding (see Fig. 3).

2.2. *In vitro* anti-proliferative activity

To investigate the *in vitro* cytotoxic properties of the Cu-N, N-CipA complexes, concentrations which induced 50% inhibition of cellular proliferation (IC$_{50}$) across two cancerous cell lines at 24 and 72 h time points were first determined *via* the colorimetric MTT assay.[27] Sigmoidal dose–response curves were plotted and concentrations which inhibited 50% cellular proliferation (IC$_{50}$ values) were determined *via* statistical analysis at the 95% confidence interval. The human breast adenocarcinoma cell line (MCF-7) and the human prostate carcinoma cell line (DU145) were chosen on the basis they are amongst the most common cancer diagnoses (according to estimated new cases in 2018) as listed by the National Cancer Institute.[28] MCF-7 are also an example of slow-growing cells as well as being poorly responsive to some copper(II) complexes described in the literature.[29] Furthermore, the DU145 cell line was also selected because these cells possess a mutant p53 gene[30] and modifications in its expression can lead to transcriptional activation of p21 and p73, which results in apoptosis. Mutations in the TP53 gene which encodes for the p53 tumour suppressor, are the most commonplace alterations in human cancer. Mutant p53 cannot bind DNA in an effective way, leading to the p21 protein not being available to act as the 'stop signal' for cell division.[31] According to the International Agency for Research on Cancer there appears to be more than 26 000 somatic mutations of p53.[32] As a representative control, we compared the cytotoxicity of our complexes to that of doxorubicin (US trade name Adriamycin) due to its known DNA-damaging properties and an ability to inhibit topoisomerase II.[33]

As reported in the literature, doxorubicin shows high cytotoxicity after 24 h against MCF-7 and DU145 cell lines with IC$_{50}$ values of 1.44 ± 0.28 and 0.15 ± 0.02 μM respectively, Table 1.[9a] Its cytotoxicity is enhanced following an additional 48 h of incubation (72 h in total) with IC$_{50}$ values of 0.94 ± 0.19 and <1.25 μM against MCF-7 and DU145, respectively. After 24 h drug treatment, the complexes showed excellent *in vitro* cytotoxicity with low μM IC$_{50}$ values observed ranging from 2.12–7.43 μM against MCF-7 and 3.27–5.59 μM against DU145 cells, Table 1. The order of activity after 24 h exposure in the MCF-7 cell line was Cu-DPPZ-CipA > Cu-DPQ-CipA > Cu-phen-CipA. In DU145 cells, the most active complex after 24 h drug exposure was also shown to be Cu-DPPZ-CipA, followed by Cu-phen-CipA and Cu-DPQ-CipA. Post 24 h drug exposure, a shift in IC$_{50}$ values from higher to lower values was observed for all complexes tested in both cell lines. After 72 h the Cu-DPPZ-CipA complex was particularly cytotoxic, exhibiting nanomolar *in vitro* cytotoxic activity (0.88 ± 0.05 μM) in the MCF-7 cell line. In addition, IC$_{50}$ values for Cu-DPQ-CipA and Cu-phen-CipA decreased by a factor of 2. A similar trend was observed in the DU145 cell line after 72 h. The most active complex was again Cu-DPPZ-CipA (1.89 ± 0.33 μM). The other two complexes, Cu-phen-CipA and Cu-DPQ-CipA, exhibited comparable cytotoxicities. CipA showed activity greater than 100 μM after 24 h treatment in both cell lines. However, this

Table 1 *In vitro* cytotoxicity data (IC$_{50}$ values) toward MCF-7 and DU145 cell lines

IC$_{50}$[a] (μM)				
	MCF-7		DU145	
Compound	24 h	72 h	24 h	72 h
Cu-phen-CipA	7.43 ± 0.99	3.05 ± 0.49	5.33 ± 0.70	2.04 ± 0.32
Cu-DPQ-CipA	7.00 ± 0.57	3.13 ± 0.25	5.59 ± 0.28	2.09 ± 0.51
Cu-DPPZ-CipA	2.12 ± 0.41	0.88 ± 0.05	3.27 ± 0.46	1.89 ± 0.33
CipA	>100	75.32 ± 3.08	>100	35.95 ± 2.51
Doxorubicin[9a]	1.44 ± 0.28	0.94 ± 0.19	0.15 ± 0.02	<1.25
[Cu(phen)$_2$]$^{2+}$	6.60 ± 0.60	0.73 ± 0.05	1.73 ± 0.35	0.80 ± 0.19

[a] Data represents mean ± SD of the results of three separate determinations; IC$_{50}$ (μM) ± SD.

decreased after 72 h of incubation with IC_{50} values for the ligand alone of 75.32 ± 3.08 μM and 35.95 ± 2.51 μM for MCF-7 and DU145, respectively. A summary of the *in vitro* cytotoxicity data is presented in Table 1.

2.3. DNA binding affinity

Complex binding to double strand DNA (dsDNA) was studied using competitive ethidium bromide (EtBr) fluorescence displacement on ctDNA, ultrahigh purity using a previously published method.[34] Binding activity was confirmed using a second polymer, salmon testes DNA (stDNA), the details of which are included in ESI.† Quenching analysis of Hoechst 33258 (groove binder) and EtBr (intercalator) were also employed to identify the binding mode.

A high throughput competitive EtBr displacement assay was employed in which an optimised mixture of ctDNA (10 μM) and EtBr (12.6 μM) was incubated for 1 h with added quencher ([drug]) in a total volume of 100 μL buffer, Fig. 4. The fluorescent quenching study, in contrast, comprised ctDNA (50 μM) and EtBr (10 μM) or Hoechst 33258 in HEPES buffer (80 mM) with added drug, Fig. 5. Measurements were conducted using excitation and emission filters of 360 and 460 nm for Hoechst 33258 and 530 and 590 nm for EtBr. A reduction in fluorescence, upon treatment with drug, was indicative of displacement of EtBr bound to DNA. Actinomycin D and netropsin were used as reference standards due to their known intercalative and minor groove binding properties, respectively. Apparent ctDNA binding constants are reported in Table 2 (A).

The DNA binding constant (K_{app}) for $[Cu(phen)_2]^{2+}$ was 6.67×10^5 M^{-1}, Table 2 (A), consistent with literature reports.[34] Interestingly, replacement of one phen ligand with CipA enhanced DNA binding by one order of magnitude. The presence of the phenazine ligands, DPQ and DPPZ, in the Cu-N,N-CipA complexes, were found to significantly enhance DNA binding with calculated K_{app} values of *ca.* 1.3×10^7 $M(bp^{-1})$ and *ca.* 1.0×10^7 $M(bp^{-1})$ respectively, similar to the K_{app} of actinomycin D (a known intercalator), Table 2 (A), under these conditions.[3a] In fact, these K_{app} values are akin to the cationic-phenazine functionalised Cu-phen complexes reported by Kellett *et al.*[8] Quenching studies (Fig. 5, Table 2 (B)) suggest that the Cu-N,N-CipA complexes displace DNA-bound Hoechst to a higher extent than EtBr, Table 2 (B). Reports in the literature suggest that Q values >20 μM in EtBr quenching studies

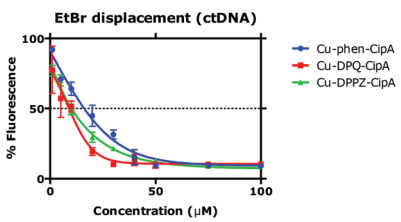

Fig. 4 Competitive EtBr displacement assays with ctDNA. Data points are presented as an average of triplicate measurements ± SD. Data points for CipA are omitted for clarity.

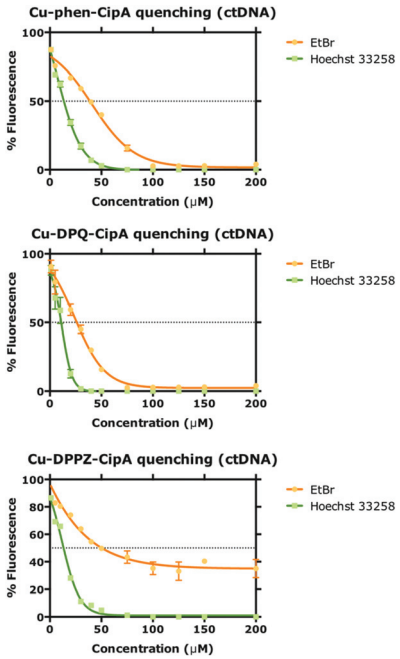

Fig. 5 Competitive EtBr displacement: Fluorescence quenching of limited bound EtBr intercalator and Hoechst 33258 displacement assays with ctDNA. Data points are presented as an average of triplicate measurements ± SD. Data points for CipA are omitted for clarity.

on ctDNA are indicative of 'classical' DNA intercalation. In contrast, minor groove binders have Q values between 2–15 μM.[35] We can deduce from our data that the Cu-N,N-CipA complexes appear to either intercalate (DPPZ and DPQ) or semi-intercalate (phen) DNA *via* the minor groove, Table 2 (B). As expected, no significant quenching was observed for CipA at concentrations greater than 300 μM.

To investigate if the redox state of the copper ion was important for the EtBr displacement induced by these complexes, assays were repeated but in the presence of 3 equivalents of reductant (Na-L-ascorbate) over a wide range of time points and over a wide concentration range. The results indicated that only Cu-DPQ-CipA reached 50% reduction in fluorescence within the first 5 min. In contrast, the DPPZ and phen analogues did not reach 50% displacement over this concentration range nor over this time period, Fig. S9 (ESI†). These results indicate that, upon reduction to copper(I), the complexes do not significantly affect EtBr displacement suggesting therefore that the 2+ oxidation state is crucial for the binding and intercalating properties observed for these complexes. This change in electrostatic charge from 2+ to 1+ may possibly diminish DNA binding activity and account for the decrease in fluorescence observed when the experiments were repeated in the presence of the reducing agent.

2.4. Topoisomerase activity

Human topoisomerases are multifunctional enzymes that relieve topological constraints in DNA during processes including chromatin assembly, recombination and chromosome seg-

Table 2 (A) Apparent ctDNA binding constants (K_{app}) as determined by competitive EtBr competitive quenching, (B) fluorescence quenching (Q) values obtained using ctDNA bound with Hoechst 33258 (groove binder) or EtBr (DNA intercalator)

	(A)		(B)	
Compound	C_{50} [a] (μM)	K_{app} [b] $(M(bp)^{-1})$	Q[c] Hoechst 33258 (μM)	Q[d] EtBr (μM)
Actinomycin D	4.10	2.92×10^7	26.34	4.78
Netropsin	46.27	2.50×10^6	2.40	20.04
$[Cu(phen)_2]^{2+}$	179.21	6.67×10^5	34.96	20.83
CipA	>300 (>300)	NC	>300 (>300)	>300 (>300)
Cu-phen-CipA	16.23 (17.35)	7.38×10^6 (6.90×10^6)	14.94 (18.32)	41.56 (41.05)
Cu-DPQ-CipA	8.99 (9.31)	1.33×10^7 (1.29×10^7)	12.19 (12.45)	48.38 (49.93)
Cu-DPPZ-CipA	10.62 (13.26)	1.13×10^7 (9.03×10^6)	14.40 (13.02)	51.49 (48.67)

[a] C_{50} is the concentration required to reduce fluorescence by 50%. [b] $K_{app} = K_e \times 12.6/C_{50}$ where $K_e = 9.5 \times 10^6$ $M(bp)^{-1}$; values in brackets represent stDNA data. NC = not calculated. [c] Q = displacement of 50% initial fluorescence from DNA-bound dye. [d] Q = concentration required to effect 50% removal of the initial fluorescence of bound dye.

regation by making transient single- (topo I) or double-strand (topo II) DNA breaks.[36] DNA topoisomerases (topo) are considered to be the main target of quinolones. In addition, quinolones can be considered as topoisomerase poisons as they have the ability to convert gyrase and topoisomerase IV (two type II topoisomerases) into cellular toxins.[37] A recent study where serine and acidic residues of topoisomerase were in close proximity to the quinolone structure, showed that the distance between the amino acids and the quinolone was too great to facilitate binding. On the other hand, a structure of a magnesium–quinolone complex incorporating four molecules of water which had non-catalytic magnesium(II) bound to the quinolone over the *C*3/*C*4 keto acid, confirmed that the co-ordinated water molecules could interact with the serine and acidic residues *via* hydrogen bonding interactions.[38] The presence of a metal ion–water complex suggests that serine and acidic residues act as anchor points which enhance the coordination of the bridge to the enzyme and that the water–metal ion bridge is the primary interaction between the drug and bacterial type II enzymes.[39] Importantly, serine and acidic residues needed to affix this water–metal ion bridge are not present in human type II topoisomerase, leading to the elimination of this key mechanism, making the toxicity of quinolones negligible for humans.[39,40]

The topoisomerase I mediated DNA relaxation assay was employed to probe the DNA binding properties of the Cu-N,N-CipA series. Cu-phen-CipA was found to induce complete relaxation of negatively supercoiled DNA (–) to the open circular form (0) at 50 μM with positive supercoiling (+) occurring thereafter. When the ligated N,N ligand was systematically extended from 1,10-phenanthroline to DPQ and further extended to DPPZ, the concentration required to relax scDNA reduces to 5.0 and 2.5 μM respectively with an increase in DNA damage observed at higher loading values. All complexes within this series were identified to intercalate (DPQ and DPPZ) or semi-intercalate (phen) and unwind negatively supercoiled plasmid DNA inhibiting topoisomerase I enzymatic activity with the overall trend: Cu-DPPZ-CipA > Cu-DPQ-CipA > Cu-phen-CipA. Designer phenazine systems in the Cu-N,N-CipA model had a significant impact on the inhibition of

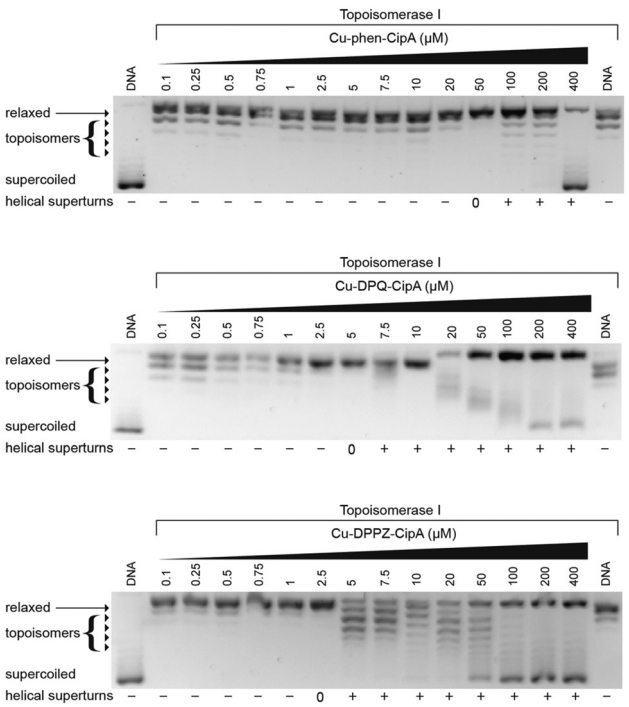

Fig. 6 Topoisomerase I mediated DNA relaxation in the presence of Cu-N,N-CipA complexes (where N,N = phen, DPQ or DPPZ). Negatively supercoiled (SC) pUC19 was initially incubated with increasing concentrations of each complex (0.1–400 μM) prior to treatment with topoisomerase I. The positive (+), relaxed open circular (0) and negative (–) helical superturns are presented below the gels.

the topoisomerase I enzyme as the concentration required to relax scDNA when compared to Cu-phen-CipA, Fig. 6.

2.5. Chemical nuclease activity

The ability of the complexes to cleave DNA was also assessed, in the presence and absence of reactive oxygen species (ROS) scavengers, using electrophoretic mobility shift assays on supercoiled (FI, bottom band) pUC19 DNA, Fig. 7. The chemical nuclease activity of the complexes was compared to that of $[Cu(phen)_2]^{2+}$ which we have previously reported.[9a] The pro-

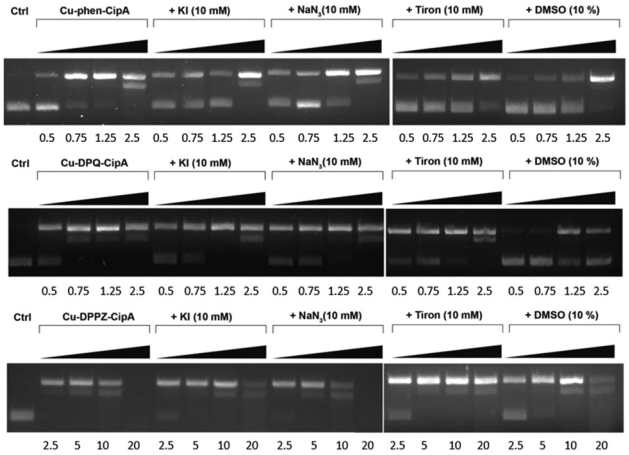

Fig. 7 DNA cleavage reactions with complexes from the series in the presence or absence of ROS specific scavengers: 400 ng of SC pUC19 was incubated for 30 min at 310 K with concentrations of 0.5 (lane 1), 0.75 (lane 2), 1.25 (lane 3) and 2.5 μM (lane 4) Cu-phen-CipA/Cu-DPQ-CipA; 2.5 (lane 1), 5 (lane 2), 10 (lane 3) and 20 μM (lane) Cu-DPPZ-CipA; in the presence of 25 mM NaCl, 0.5 mM Na-L-ascorbate and 80 mM HEPES.

cedure employed was adapted from a previously reported method.[41] Briefly, in these experiments, 400 ng of pUC19 DNA was incubated for 30 min with drug concentrations ranging from 0.5–2.5 μM for Cu-phen-CipA and Cu-DPQ-CipA and 2.5–20 μM for Cu-DPPZ-CipA, in the presence or absence of ROS scavengers/stabilisers, before being quenched and examined using agarose gel electrophoresis. The concentrations of the test complexes were optimised in which a degradation profile could be visualised and representative DNA bands of single strand damage (open circular, FII, below top band) and double strand damage (linear, FIII, top band) could be identified, Fig. 7. The scavengers employed were: KI (10 mM) as a H_2O_2 scavenger, NaN_3 (10 mM) as $^1O_2$ scavenger, DMSO (10%) as $^{\bullet}OH$ scavenger and tiron (4,5-dihydroxy-1,3-benzenedisulfonic acid disodium salt or TH_2) as $O_2^{\bullet-}$ scavenger (10 mM).

We previously reported that the nuclease activity of $[Cu(phen)_2]^{2+}$, in the presence of TH_2, was found to be significantly hindered with cleavage of SC FI pUC19 DNA to FII and FIII at 1.0 and 2.5 μM. The $^{\bullet}OH$ scavenger, DMSO, was found to have a similar effect on cleavage activity at these concentrations while incubation with KI and NaN_3 had only marginal effects. It was concluded from this study that the predominant ROS responsible for the observed DNA cleavage were $O_2^{\bullet-}$ and $^{\bullet}OH$.[9a]

All three complexes were found to likewise exhibit excellent nuclease activity, Fig. 7. The Cu-phen-CipA and Cu-DPPZ-CipA complexes possessed lower nuclease activity if compared to $[Cu(phen)_2]^{2+}$, where complete degradation of FI to FII and FIII was observed at 2.5 μM. Significantly, Cu-DPQ-CipA showed complete degradation of FI to FII and FIII at 0.75 μM, making it the most efficient nuclease activator in the series. In the case of Cu-DPPZ-CipA, the main ROS involved in DNA damage were both $O_2^{\bullet-}$ and $^{\bullet}OH$ where TH_2 and DMSO significantly inhibited the cleavage efficiency of FI to FII and FIII at 2.5 μM. In addition, DMSO and TH_2 were also the scavengers that exhibited an inhibition of chemical nuclease activity of Cu-DPQ-CipA possibly indicating that $^{\bullet}OH$ and $O_2^{\bullet-}$ species were involved in inducing DNA damage for this complex also. However, DMSO proved to be the best scavenger of the series, suggesting that $O_2^{\bullet-}$ is most likely the predominant ROS that mediates DNA damage. Furthermore, the Cu-phen-CipA was the only complex in the series that showed all four ROS being important for its nuclease activity – complete degradation of FI to FII and FIII observed at 1.25 μM could be inhibited with all four ROS scavengers. Of note is the fact that the presence of the CipA in these complexes did not adversely impact on their ability to induce significant nuclease activity.

2.6. *In vitro* bactericidal and fungicidal activity

The bactericidal and fungicidal activity of the ligands and complexes toward a range of Gram positive (*Staphylococcus aureus* (SA); methicillin resistant *Staphylococcus aureus* (MRSA); *Enterococcus* sp. (EF) and *Staphylococcus epidermidis* (SE)) and Gram negative bacteria (*Escherichia coli* (EC); *Klebsiella pneumoniae* (KP); *Klebsiella pneumoniae* ESBL positive (KP-E) and *Pseudomonas aeruginosa* (PA)) were examined along with their effect on non-filamentous fungi (*Candida albicans* ATCC 44859 (CA1); *Candida albicans* ATCC 90028 (CA2); *Candida parapsilosis* ATCC 22019 (CP); *Candida krusei* ATCC 6258 (CK1); clinical yeast isolates (*Candida krusei* E28 (CK2); *Candida tropicalis* 156 (CT); *Candida glabrata* 20/I (CG); *Candida lusitaniae* 2446/I (CL); *Trichosporon asahii* 1188 (TA)), and filamentous fungi (*Aspergillus fumigatus* 231 (AF); *Absidia corymbifera* 272 (AC) and *Trichophyton mentagrophytes* 445 (TM)), Tables 3 and 4.

Briefly, the activity of the phenazine ligands, the Cu-N,N-CipA complexes and Cip ligand were tested at 24 and 48 h time points across the above mentioned panel of bacteria and fungi. The exception was *Trichophyton mentagrophytes* 445 (TM) which was tested at 72 and 120 h. Due to solubility issues, the minimum inhibitory concentrations that induce 95% bacterial growth inhibition (MIC_{95}) of CipA could not be evaluated as the desired concentration needed for these experiments could not be achieved. The anti-microbial activity of Cip, however, was as expected with MIC_{95} values ranging from 1.95–3.9 μM against SA, 0.98–1.95 μM against EC and KP and 3.9–7.81 μM against EF at 24 h and 48 h, respectively. No significant activity was observed against MRSA, SE and KP-E with MIC_{95} values of 125 μM. The activity of phen, DPQ and DPPZ varied with MIC_{95} values ranging from 3.90–2000 μM. The DPPZ ligand exhibited greatest potency with MIC_{95} values ranging from 3.90, 7.81 and 15.62 μM against SE, SA and MRSA strains respectively.

The most active complexes in the series were Cu-phen-CipA and Cu-DPPZ-CipA with MIC_{95} ranging from 7.81–31.25 μM across the Gram positive strains. The complexes exhibited moderate to poor activity against the Gram negative strains (MIC_{95} values ranging from 31.25 to >125 μM), suggesting that these Cu-N,N-CipA complexes selectively target Gram positive bacteria. Interestingly, although all the Cu-N,N-CipA complexes were more potent against MRSA and SE relative to Cip, the Cu-DPPZ-CipA complex was most potent, with a MIC_{95} of

Table 3 *In vitro* bactericidal activity data (MIC_{95}) towards Gram-positive and Gram-negative bacterial strains

MIC_{95} (μM)																
	Gram positive bacteria[a]								Gram negative bacteria[b]							
	SA		MRSA		SE		EF		EC		KP		KP-E		PA	
Compound	24 h	48 h	24 h	48 h	24 h	48 h	24 h	48 h	24 h	48 h	24 h	48 h	24 h	48 h	24 h	48 h
phen	125	ND	500	ND	1000	ND	62.5	ND	2000	ND	1000	ND	1000	ND	2000	ND
DPQ	62.5	62.5	62.5	125	125	125	62.5	62.5	250	500	500	500	5000	500	500	500
DPPZ	7.81	7.81	7.81	15.62	3.90	3.90	125	250	500	500	500	500	500	500	500	500
$[Cu(phen)_2]^{2+}$	31.25	31.25	15.62	15.62	62.5	62.5	15.62	15.62	62.5	62.5	62.5	62.5	62.5	62.5	1000	1000
Cu-phen-CipA	15.62	15.62	31.25	31.25	31.25	31.25	62.5	62.5	62.5	62.5	>125	>125	>125	>125	>125	>125
Cu-DPQ-CipA	7.81	31.25	31.25	31.25	62.5	125	62.5	125	>125	>125	>125	>125	>125	>125	>125	>125
Cu-DPPZ-CipA	7.81	15.62	15.62	15.62	15.62	15.62	31.25	62.5	>125	>125	>125	>125	>125	>125	>125	>125
Cip	1.95	3.9	125	125	125	125	3.9	7.81	0.98	1.95	0.98	1.95	125	125	31.25	31.25

[a] *Staphylococcus aureus* (SA), methicillin resistant *Staphylococcus aureus* (MRSA), *Staphylococcus epidermidis* (SE) and *Enterococcus* sp. (EF). [b] *Escherichia coli* (EC), *Klebsiella pneumoniae* (KP), *Klebsiella pneumonia* ESBL positive (KP-E) and *Pseudomonas aeruginosa* (PA). ND = not determined.

Table 4 *In vitro* fungicidal activity data towards non-filamentous fungi (MIC_{80}) and towards filamentous fungi (MIC_{50}). MIC_{50} of TM strain was determined at 72 and 120 h, whereas MIC_{50} of all other strains were determined at 24 and 48 h

	Non-filamentous fungi (ATCC strains)[a] – MIC_{80} (μM)								Non-filamentous fungi (clinical yeast isolates)[b] – MIC_{80} (μM)										Filamentous fungi[c] – MIC_{50} (μM)					
	CA1		CA2		CP		CK1		CK2		CT		CG		CL		TA		AF		AC		TM	
Compound	24 h	48 h	24 h	48 h	24 h	48 h	24 h	48 h	24 h	48 h	24 h	48 h	24 h	48 h	24 h	48 h	24 h	48 h	24 h	48 h	24 h	48 h	72 h	120 h
phen	7.81	ND	7.81	ND	ND	ND	7.81	ND	7.81	ND	31.25	ND	7.81	ND	15.62	ND	7.81	ND	15.62	15.62	15.62	15.62	7.81	7.81
DPQ	31.25	31.25	31.25	31.25	31.25	31.25	62.5	62.5	62.5	62.5	125	125	31.25	125	31.25	31.25	31.25	31.25	62.5	62.5	31.25	31.25	31.25	31.25
DPPZ	62.5	500	62.5	500	500	500	500	500	500	500	500	500	62.5	500	500	500	7.81	7.81	500	31.25	500	500	500	500
$[Cu(phen)_2]^{2+}$	15.62	15.62	15.62	15.62	15.62	15.62	7.81	7.81	15.62	15.62	31.25	31.25	15.62	15.62	7.81	7.81	15.62	15.62	31.25	31.25	31.25	31.25	15.62	15.62
Cu-phen-CipA	125	125	125	125	125	125	62.5	62.5	62.5	62.5	125	125	125	125	>125	>125	125	125	>125	>125	>125	>125	>125	>125
Cu-DPQ-CipA	125	125	125	125	125	125	31.25	31.25	31.25	31.25	>125	>125	>125	>125	62.5	62.5	>125	>125	>125	>125	>125	>125	>125	>125
Cu-DPPZ-CipA	>125	>125	>125	>125	>125	>125	15.62	15.62	15.62	15.62	62.5	62.5	62.5	62.5	31.25	31.25	>125	>125	>125	>125	>125	>125	>125	>125
Cip	>125	>125	>125	>125	>125	>125	>125	>125	>125	>125	>125	>125	>125	>125	>125	>125	>125	>125	>125	>125	>125	>125	>125	>125

[a] *Candida ablicans* ATCC 44859 (CA1), *Candida ablicans* ATCC 90028 (CA2), *Candida parapsilosis* ATCC 22019 (CP) and *Candida krusei* ATCC 6258 (CK1). [b] *Candida krusei* E28 (CK2), *Candida tropicalis* 156 (CT), *Candida glabrata* 20/I (CG), *Candida lusitaniae* 2446/I (CL) and *Trichosporon asahii* 1188 (TA). [c] *Aspergillus fumigatus* 231 (AF), *Absidia corymbifera* 272 (AC) and *Trichophyton mentagrophytes* 445 (TM). ND = not determined.

15.62 μM in contrast to Cip which had an MIC_{95} of 125 μM against the same strain. Methicillin-resistant *S. aureus* or MRSA is known to be a major causative agent of community-acquired infections.[42] Antibiotic resistance in *S. aureus* has also become a major challenge. According to a report recently released by the World Health Organization (WHO), most antibiotic agents under development are modifications of existing antibiotics.[43] They highlight the need to develop innovative approaches to cater for the anticipated further evolution of resistance. Combining antibiotics with metal ions such as copper(II) may represent an innovative approach in this field and already some groups are advancing this line of research.[44] From our findings, the Cu-N,N-CipA derivatives may serve as potential new leads. Their mode of bactericidal activity thus warrants further investigation. A summary of the *in vitro* bactericidal activity of the Cu-N,N-CipA derivatives is presented in Table 3 and Fig. 8.

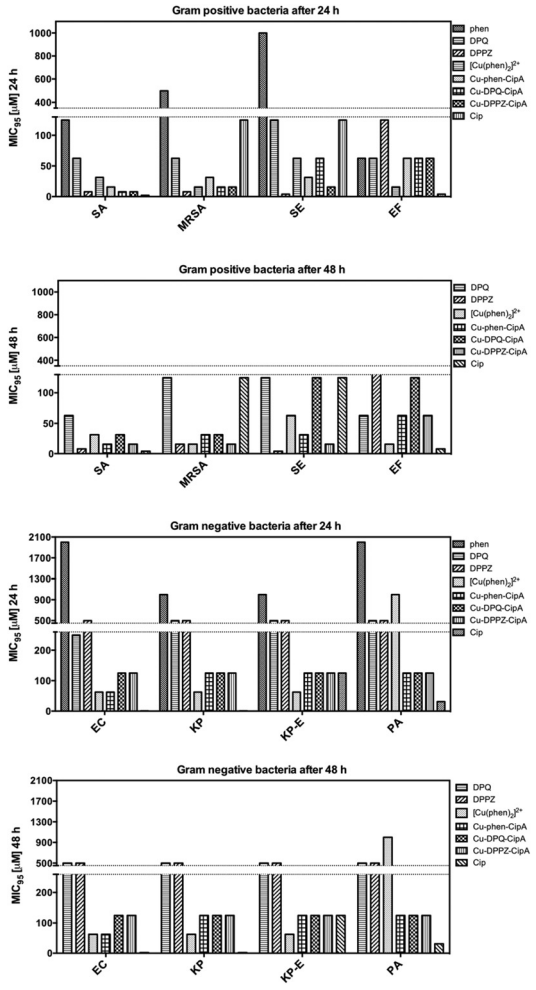

Fig. 8 Bactericidal activity of the N,N-ligands, Cip and Cu-N,N-CipA derivatives across a panel of Gram positive ((*Staphylococcus aureus* (SA); methicillin resistant *Staphylococcus aureus* (MRSA); *Enterococcus* sp. (EF) and *Staphylococcus epidermidis* (SE)) and Gram negative bacteria (*Escherichia coli* (EC); *Klebsiella pneumoniae* (KP); *Klebsiella pneumoniae* ESBL positive (KP-E) and *Pseudomonas aeruginosa* (PA)).

While Cip demonstrated potent bactericidal activity in a number of Gram positive and Gram negative bacterial strains, Table 3, it exhibited no fungicidal activity in all fungal strains tested, with determined MIC_{50} and MIC_{80} values >125 μM in all cases. In contrast to the anti-bacterial properties, the *in vitro* anti-fungal activity of the metal-free phen ligand surpassed that of all of the complexes tested, with consistent MIC_{50} and MIC_{80} values ranging from 7.81–15.62 μM in all the fungal strains tested. This observation is in agreement with previously published results,[3c] most likely due to the ability of this ligand to bind trace metal ions (*e.g.* zinc(II)) which are essential for fungal survival. The $[Cu(phen)_2]^{2+}$ complex exhibited broad spectrum anti-fungal activity across the panel line tested. The Cu-N,N-CipA complexes, in contrast, showed little anti-fungal activity towards the panel tested, with the exception of Cu-DPPZ-CipA which had an MIC_{80} of 15.62 μM toward the CK1 and CK2 strains and an MIC_{80} of 31.25 μM toward the CL strain. A summary of the *in vitro* fungicidal activity of the Cu-N,N-CipA derivatives is presented in Table 4 and Fig. S10 (ESI†).

2.7. *In vivo* toxicity using *Galleria mellonella*

The immune system of insects bears remarkable functional and structural similarities to that of the innate immune system of mammals.[45] As such, insects may be employed as models for studying the virulence of human pathogens[46] and for assessing the *in vivo* efficacy of novel anti-microbial drugs.[47] Larvae of the greater wax moth, *G. mellonella*, have been successfully employed for this purpose. Numerous studies have indicated a strong correlation between results obtained using this insect model and those obtained using mammals.[46,48] Larvae of *G. mellonella*, for example, have been successfully utilised for assessing the toxicity of food preservatives[49] and, of particular note, novel silver based anti-cancer drugs.[50]

The effect of the Cu-phen-CipA, Cu-DPQ-CipA and Cu-DPPZ-CipA complexes and the CipA ligand on the viability of *G. mellonella* larvae was therefore assessed, Fig. 9. The larvae were administered test solutions by injection directly into the haemocoel through the last pro-leg across a concentration range from 50–1000 μg mL^{-1}. Larvae survival was monitored after 24, 48 and 72 h of test compound exposure and death noted by their lack of movement in response to a stimulus and cuticle discoloration.

The CipA and all complexes tested were well tolerated by the larvae, Fig. 9. Of the complex series, the Cu-DPQ-CipA was the least toxic with no kill observed after 72 h exposure across the concentration range. The Cu-phen-CipA complex was found to be the most toxic at the highest concentration tested (1000 μg mL^{-1}) with *ca.* 30% kill after 24 h of exposure. The Cu-DPPZ-CipA complex was shown to be less toxic at the same time point and also at the highest concentration with *ca.* 23% kill. After a further 48 h of exposure (72 h in total), the Cu-phen-CipA complex induced further death (*ca.* 36%) while Cu-DPPZ-CipA remained unchanged. At the same time point (72 h) of exposure at the lowest tested concentration, 7–10% of larvae were killed in the case of Cu-DPQ-CipA, Cu-DPPZ-CipA and CipA. However, this can occur often due to an infection

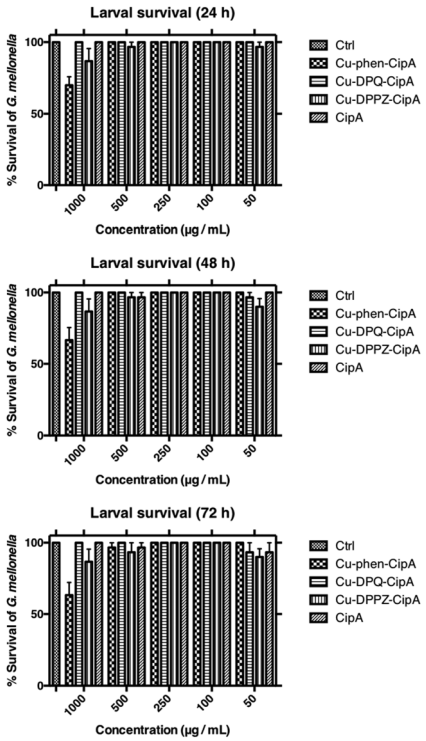

Fig. 9 % Survival of *G. mellonella* exposed to different agents for 24 h, 48 h and 72 h. Data represent mean ± SEM of the results of three separate determinations.

and may not necessarily correlate with these test agents. These results provide preliminary evidence that the Cu-N,N-CipA complexes are well tolerated by the larvae which bodes well for their general *in vivo* toxicity profile.

3. Conclusions

We have successfully employed a one-pot synthetic protocol to generate a library of copper(II) complexes of general formula [Cu(N,N)(CipA)Cl] where N,N represents a phenanthrene ligand and CipA, a derivative of the clinically used fluoroquinolone antibiotic ciprofloxacin. These complexes were rationally designed so as to incorporate a Cu-N,N-framework with DNA binding and DNA oxidant properties and an antibiotic derivative with known anti-proliferative and anti-microbial activities. Based on X-ray structural analysis, the [Cu(Phen)(CipA)Cl] complex exists in a slightly distorted square pyramidal geometry with the copper(II) ion coordinated by two CipA O atoms and two phen N atoms in the equatorial plane, and by a Cl ion in the axial position. Of the complex series, the quinoxaline and phenazine complexes, Cu-DPQ-CipA and Cu-DPPZ-CipA, exhibited excellent DNA binding affinities with K_{app} values in the 10^7 M(bp)$^{-1}$ range. All complexes appeared to intercalate DNA *via* minor groove interactions and to mediate DNA damage by generating ROS with superoxide and hydroxyl free radicals playing crucial roles in DNA strand scission. The complexes were highly cytotoxic against a human breast adenocarcinoma (MCF-7) and a human prostate carcinoma cell line (DU145), the latter being p53 null, with low micromolar cytotoxicities observed after 24 h of treatment in contrast to CipA (IC_{50} > 100 μM). The Cu-DPPZ-CipA complex, in particular, was found to be highly cytotoxic (nanomolar range) against the breast carcinoma cells after 72 h. Given that topoisomerases are one of the main targets of fluoroquinolone antibiotics, the complexes were assessed for their topoisomerase inhibitory activity. Of the series, the Cu-DPPZ-CipA complex exhibited the greatest inhibitory activity. Furthermore, the complexes appear to selectively target Gram positive bacteria over Gram negative bacteria with Cu-DPPZ-CipA having an order of magnitude greater potency against Methicillin-resistant *S. aureus* (MRSA) as compared to the free CipA ligand. In addition, the CipA ligand and all the complexes tested were well tolerated by a widely adopted *in vivo* insect model which bodes well for their future development as drugs. Taking all these facts into consideration, these complexes, but particularly Cu-DPPZ-CipA as the lead drug candidate, have significant potential to act as novel prophylactic metallo-antibiotics for the treatment of cancer patients at high risk of infection and thus warrant further investigation. Given that antibiotic resistance in *S. aureus* has become a major challenge, there is an urgent need to identify new approaches to cater for the anticipated further evolution of resistance. These complexes may thus also offer promise as metallo-antibiotics in their own right.

4. Experimental section

4.1. Materials and methods

EtBr, netropsin, actinomycin D, DMF and Hoechst 33258 were purchased from Sigma-Aldrich (Arklow, Ireland) and used as received. pUC19 vector (N3041) was purchased from New England Bio-Labs (NEB), UltraPure Calf Thymus DNA from Invitrogen (ctDNA, ε_{260} = 12 824 M(bp)$^{-1}$ cm^{-1}) and salmon testes DNA from Sigma Aldrich Ireland (stDNA, ε_{260} = 13 423 M(bp)$^{-1}$ cm^{-1}). NaCl and HEPES were obtained from Ambion while 1 M HEPES buffer (pH 7.2) was purchased from Fisher Scientific. 1,10-Phenanthroline-5,6-dione (phendione), DPQ and DPPZ were prepared as previously reported in literature.[8] ^{1}H and ^{13}C spectra were recorded using a Bruker DPX 400 spectrometer (room temperature; 400 MHz and 101 MHz, respectively). Coupling constants (J) are quoted in Hz. The splitting of the proton resonances is labelled as s = singlet, d = doublet, t = triplet, sept = septet, m = multiplet. Chemical shifts (δ) are quoted in parts per million (ppm) using residual protons in the indicated solvents as internal standards. NMR data processing was carried out using MestReNova, version 6.0.2-5475. Infrared spectra were recorded on a Bruker Tensor 27 spectrometer with KBr as a standard. IR spectra were analysed using OPUS, version 5.0, with peak positions (ν) in cm^{-1}. Mass spectrometry was carried out on an Advion Expression Compact Mass Spectrometer: 10 μL of the samples were

injected in 300 μL of methanol : water : formic acid (90 : 9 : 1 v/v). Microanalysis was carried out at the Department of Chemistry, University College Dublin.

4.2. Syntheses

The ligands 1,10-phenanthroline-5,6-dione (phendione), dipyrido[3,2-*f*:2′,3′-*h*]quinoxaline (DPQ), dipyrido[3,2-*f*:2′,3′-*h*]quinoxaline (DPQ) and dipyrido[3,2-*a*:2′,3′-*c*]phenazine (DPPZ) were prepared according to previously prublished methods.[8]

4.2.1. Synthesis of [Cu(1,10-phen)(CipA$_{-H}$)Cl] (Cu-phen-CipA). $CuCl_2{\cdot}2H_2O$ (70.2 mg, 0.412 mmol, 1 eq.) was dissolved in water (6 mL) and a hot solution of phen (74.2 mg, 0.412 mmol, 1 eq.) in EtOH (10 mL) added. To this was added previously dissolved CipA (200 mg, 0.412 mmol, 1 eq.) in MeOH (15 mL) with NaOH (16 mg, 0.412 mmol, 1 eq.) in water (2.5 mL). The pH was adjusted to *ca.* 8 with 0.2 M NaOH. The round bottom flask was sealed with parafilm and left to stir at room temperature overnight. The flask was left open at room temperature and after two days turquoise to dark green crystals were deposited. Crystals were isolated by filtration and dried in a desiccator to yield dark green crystals (0.316 mmol, 77%). ESI-MS (positive mode; MeOH) *m*/*z* 762.23 [M], 727.02 $[M - Cl]^+$. IR selected bands (cm^{-1}, KBr): 2914, 2851, 1620, 1588, 1515, 1478, 1303, 1250, 1224, 1025, 945, 858, 726 cm^{-1}. Anal. Calcd for $C_{39}H_{43}ClCuFN_5O_4{\cdot}3H_2O$: C, 57.28; H, 6.04; N, 8.56; Cu, 7.77. Found: C, 57.14; H, 5.70; N, 8.30; Cu, 7.39.

4.2.2. Synthesis of [Cu(DPQ)(CipA$_{-H}$)Cl] (Cu-DPQ-CipA). $CuCl_2{\cdot}2H_2O$ (35.1 mg, 0.206 mmol, 1 eq.) was dissolved in water (4 mL) and a hot solution of DPQ (47.8 mg, 0.206 mmol, 1 eq.) in EtOH (8 mL) added. In parallel, CipA (100 mg, 0.206 mmol, 1 eq.) was dissolved in MeOH (6 mL) followed by the addition of NaOH (8 mg, 0.206 mmol, 1 eq.) in H_2O (3 mL) and added to the Cu salt solution (~318 K). The pH was adjusted to *ca.* 8 with 0.2 M aq. NaOH. The round bottom flask was sealed with parafilm and left to stir at room temperature overnight. The following day, a green solid was isolated by filtration, washed with cold H_2O, cold MeOH and dried in a desiccator to yield a light green solid (0.098 mmol, 48%). ESI-MS (positive mode; MeOH) *m*/*z* 814.23 [M], 779.10 $[M - Cl]^+$. IR selected bands (cm^{-1}, KBr): 2920, 2853, 1613, 1579, 1523, 1477, 1383, 1301, 1247, 1083, 1023, 951, 887, 730 cm^{-1}. Anal. Calcd for $C_{41}H_{43}CuClFN_7O_4{\cdot}2H_2O{\cdot}1.5C_2H_5OH$: C, 57.38; H, 6.13; N, 10.65; Cl, 3.85. Found: 57.22; H, 5.69; N, 10.28; Cl, 3.82.

4.2.3. Synthesis of [Cu(DPPZ)(CipA$_{-H}$)Cl] (Cu-DPPZ-CipA). CipA (100 mg, 0.206 mmol, 1 eq.) was dissolved in hot MeOH (7 mL) and had an aqueous solution (2 mL) of NaOH (8 mg, 0.206 mmol, 1 eq.) added. After 5 min of stirring, $CuCl_2{\cdot}2H_2O$ (35.1 mg, 0.206 mmol, 1 eq.) dissolved in water (3 mL) and DPPZ (58.14 mg, 0.206 mmol, 1 eq.) dissolved in hot MeOH (6 mL) were added slowly and simultaneously to the CipA solution (~318 K). The pH was adjusted to *ca.* 8 with 0.2 M NaOH. The round bottom flask was sealed with parafilm and left to stir at room temperature overnight. The following day, a green solid was isolated by filtration and washed with cold H_2O, cold MeOH and dried in a desiccator resulting in a bright green solid (0.121 mmol, 59%). ESI-MS (positive mode; MeOH) *m*/*z* 864.25 [M], 829.05 $[M - Cl]^+$. IR selected bands (cm^{-1}, KBr): 2925, 2853, 1619, 1586, 1519, 1471, 1356, 1298, 1258, 1074, 1023, 949, 883, 732 cm^{-1}. Anal. Calcd for $C_{45}H_{45}ClCuFN_7O_4{\cdot}3H_2O$: C, 58.66; H, 5.18; N, 10.32; Cl, 3.32; Cu, 6.91. Found: C, 58.75; H, 5.59; N, 10.66; Cl, 3.85; Cu, 6.91.

4.3. Structure analysis of Cu-phen-CipA (8)

The X-ray structural analysis of a crystal of [Cu(phen)(CipA$_{-H}$)Cl]·$1H_2O{\cdot}1CH_3OH$ was performed on a Bruker D8 Quest Eco at 100(2) K with an Oxford Cryosystems cryostat, with samples mounted on a MiTeGen microloop using Mo Kα radiation (λ = 0.71073 Å). Bruker APEX (Bruker (2016). APEX3 v2016.9-0, Bruker AXS Inc., Madison, WI, USA) software was used to collect and reduce data and determine the space group. Absorption corrections were applied using SADABS (Bruker (2016/2). SADABS, Bruker AXS Inc., Madison, Wisconsin, USA). The structure was solved with the XT structure solution program[51] using Intrinsic Phasing and refined with the XL refinement package[52] using Least Squares minimisation in Olex2.[53] All non-hydrogen atoms were refined anisotropically. Hydrogen atoms were assigned to calculated positions using a riding model with appropriately fixed isotropic thermal parameters.

The aliphatic chain was modelled in two conformations (occupancy 52 : 48%) using restraints and constraints (SADI, EADP). The structure was refined as an inversion twin in the chiral space group $P2_12_12_1$ with a BASF of 0.100(18).

See Table 5 for crystal data and structure refinement parameters. Crystallographic data, CCDC 1586315.†

Table 5 Crystal data and structure refinement for [Cu(phen)(CipA$_{-H}$)Cl]·$1H_2O{\cdot}1CH_3OH$ (**8**)

	8
Empirical formula	$C_{40}H_{49}ClCuFN_5O_6$
fw	813.83
Crystal system	Orthorhombic
Space Group	$P2_12_12_1$
a (Å)	8.3938(4)
b (Å)	17.8033(9)
c (Å)	25.5129(11)
a (°)	90
b (°)	90
g (°)	90
V (Å^3)	3812.6(3)
T (K)	100(2)
Z	4
r (Mg cm^{-3})	1.418
m (mm^{-1})	702
Total refins	35 747
Indep. refins	7031
R (int)	0.0894
S	1.048
R_1[a] [$I > 2\sigma(I)$]	0.0442
wR_2[b] [$I > 2\sigma(I)$]	0.0862
CCDC	1586315

[a] $R_1 = \sum||F_o| - |F_c||/\sum|F_o|$. [b] $wR_2 = [\sum w(F_o^2 - F_c^2)^2/\sum w(F_o^2)^2]^{1/2}$.

4.4. Cell viability

Cells were cultured in a standard 75 cm^3 flask (Corning®, Austria) containing Roswell Park Memorial Institute medium (RPMI-1640; Sigma-Aldrich, Ireland) supplemented with 10% fetal bovine serum (Gibco®, Ireland) at 310 K in a humidified atmosphere at 5% CO_2. Cells were cultured in a mycoplasma-free facility and were routinely tested for mycoplasma contamination with MycoAlert™ Mycoplasma Detection Kit (Lonza). Every 3–4 days cells reached 70–80% confluency after which they were harvested with trypsin-EDTA (ATCC, LGC, United Kingdom) and re-suspended in media. The *in vitro* inhibition of human cancer cell line growth by means of the 3-(4,5-dimethylthiazol-2-yl)-2,5-diphenyltetrazolium bromide (MTT; Sigma-Aldrich, Belgium) colourimetric anti-proliferation assay was utilised.

Briefly, prior to addition of tested agents, MCF-7 and DU145 cells were seeded overnight in 96-well tissue culture plates (Costar) at an initial density of 4×10^5 and 2×10^5 cells per mL for 24 h and 72 h incubation points, respectively. DMSO stock suspensions of complexes were prepared at ~40 mM. Prepared stocks were further on diluted in supplemented medium to give the following final concentrations in 200 μL wells: 100, 50, 10, 5, 1, 0.5 and 0.1 μM. A DMSO control over the same concentration range was included each time. Cells grown in 96-well plates often clump towards the outer edges of the wells. This tendency, commonly called 'edge effect' was minimised by filling the inter-well spaces of a 96-well tissue culture plate with 50 μL of sterile PBS. Cells were incubated for 24 and 72 h at 310 K in a humidified atmosphere with 5% CO_2. After the desired incubation period, spent media was removed and cells were washed with PBS. 100 μL fresh media and 10 μL of 5 mg mL^{-1} MTT solution giving final concentration of 0.5 mg mL^{-1} were added followed by incubation for 3 hours at 310 K (protected from light with aluminium foil). Afterwards, all media was carefully removed, and the resulting violet formazan crystals were dissolved by addition of 150 μL of MTT solubilisation solution (0.1% Tergitol-type NP-40, 4 mM HCl and anhydrous isopropanol) for 20 min while the 96-well tissue plate was shaking. After complete dissolution of the formazan product, the absorbance was measured at 570 nm using 690 nm as the reference wavelength (background cells and proteins). IC_{50} values, as the concentration which caused 50% of cell death, were determined as duplicates of triplicate in three independent sets of experiments and their standard deviations were calculated. Cells exposed to $[Cu(phen)_2]^{2+}$ as well as untreated cells were used as positive and negative controls respectively.

4.5. *In vivo* toxicity activity using *Galleria mellonella*

G. mellonella larvae (Lepidoptera: Pyralidae, the Greater Wax Moth), in the sixth developmental stage, were used to determine the *in vivo* toxicity of CipA and the Cu-N,N-CipA complexes using a previously published methodology.[54] Larvae were obtained from the Mealworm Company in Sheffield, England and stored in wood shavings in the dark at 288 K to prevent pupation. The weight of each larvae was between 0.25–0.3 g and only healthy larvae that showed no evidence of localised melanisation or infection with no cuticle discolouration were included in the study. The experiment was carried out on three different occasions in duplicate using a group size of 10 larvae per 9 cm sterile Petri-dish. Fresh solutions of the test compounds were prepared immediately prior to testing under sterile conditions. Each compound was dissolved in 10% DMSO/PBS to give a stock solution of concentration 100 μM. All agents were tested across the concentration range 100, 10, 1 and 0.1 μM. Test solutions (20 μL) were directly injected into the haemcoel of the larvae through the last proleg – the proleg can be opened by applying gentle pressure to the sides of the larvae. This prevents damage to the larvae as this opening will re-seal following removal of the syringe needle without leaving a scar. Larvae were placed in sterile petri-dishes and incubated at 303 K for 72 h. Wood shavings were provided as a source of food. Larvae injected with sterile 10% DMSO/PBS and untreated larvae were used as controls. The survival of the larvae was monitored every 24 h. Determination of death was confirmed by the lack of movement in response to stimulus – a blunt-ended needle was used to probe the larvae. If the larvae did not respond to this stimulus, then they were considered to be non-viable or dead.

4.6. DNA binding affinity and intercalative studies

4.6.1. Competitive EtBr displacement. Competitive EtBr displacement assays were conducted using a method previously reported by Kellett *et al.*[3c,34] Briefly, a working solution of 20 μM ctDNA or stDNA; 25.2 μM EtBr; 40 mM NaCl in HEPES buffer (80 mM, pH 7.2) were prepared. Stock solutions of the Cu-N,N-CipA complexes and groove binding drugs were prepared in DMSO at ~5 mM and further diluted with 80 mM HEPES. 50 μL of a DNA-EtBr working solution were placed into each well of a 96-well micro plate, with the exception of blanks which contained 100 μL of HEPES buffer. Serial aliquots of the metal complexes and groove binding drugs were added to the working solution and the final volume was adjusted to 100 μL in each well such that the final concentrations of ctDNA or stDNA and EtBr were 10 and 12.6 μM, respectively. The plate was incubated at room temperature for 1 hour, protected from light. Microplates were analysed using a Bio-Tek synergy HT multi-mode micro plate reader with excitation and emission wavelengths set to 530/590 nm respectively. Each drug concentration was measured in triplicate and the apparent binding constants were calculated using the equation $K_{app} = K_e \times 12.6/C_{50}$, where $K_e = 9.5 \times 10^6$ $M(bp)^{-1}$.

4.6.2. Fluorescence quenching. This experiment was carried out as previously described by Kellett *et al.*[3c,8,34] A working solution of 50 μM ctDNA or stDNA along with either 10 μM EtBr or Hoechst 33258 in HEPES buffer (80 mM, pH = 7.2) and NaCl (40 mM) was prepared. Stock solutions of the Cu-N,N-CipA complexes and CipA free ligand and groove binding drugs were prepared at ~5 mM in DMSO and diluted further with 80 mM HEPES. 50 μL of DNA-EtBr or DNA-Hoechst working solutions were placed in each well of a

96-well microplate with the exception of the blanks which contained 100 μL HEPES buffer and 5 μM of either Hoechst or EtBr. Serial aliquots of the agents were added to the working solutions and the volume was adjusted to 100 μL in each well such that the final concentration of ctDNA or stDNA and EtBr/Hoechst were 25 μM and 5 μM, respectively. Each drug concentration was measured in triplicate. The plate was allowed to incubate at room temperature for 5 min before being analysed using a Bio-Tek synergy HT multi-mode micro plate reader with excitation and emission wavelengths being set to 530/590 nm for EtBr detection or 360/460 nm for Hoechst 33258 detection. Concentrations of tested compounds applied were chosen based on the fact that their fluorescence was in the range from 30–40% of the initial control at their highest reading. *Q* values can be obtained from a plot of fluorescence *versus* drug concentration and represents the concentration required to affect 50% removal of the initial fluorescence of bound dye.[34]

4.6.3. Chemical nuclease activity. The presence or absence of ROS specific scavengers were used to determine the effect on the DNA cleavage abilities of each copper complex. Briefly, in a final volume of 20 μL, 80 mM HEPES (pH = 7.2), 25 mM NaCl, 1 mM Na-L-ascorbate, and 400 ng of pUC19 DNA were treated with drug concentrations of 0.5, 0.75, 1.25 and 2.5 μM (Cu-phen-CipA and Cu-DPQ-CipA) and 2.5, 5.0, 10, 20 μM (Cu-DPPZ-CipA) in the presence or absence of ROS scavengers/stabilisers: KI (10 mM, H_2O_2 scavenger), NaN_3 (10 mM, $^1O_2$ scavenger), DMSO (10%, $^{\bullet}OH$ scavenger) and tiron (TH_2, 10 mM, $O_2^{\bullet-}$ scavenger). Reactions were incubated for 30 minutes at 310 K and quenched with 6× loading dye (Fermentas) containing 10 mM Tris-HCl, 0.03% bromophenol blue, 0.03% xylene cyanole FF, 60% glycerol and 60 mM EDTA. Samples were then loaded onto an agarose gel (1.2%) containing 3 μL of EtBr. Electrophoresis was completed within two cycles; 50 V for 30 min and 70 V for 1 h in 1× TAE buffer, respectively.

4.6.4. Topoisomerase activity. The topoisomerase I relaxation was carried out according to methods previous described with changes made to the procedure.[55] To a final volume of 20 μL; in 80 mM HEPES, 2 μL CutSmart buffer (NEB, B7204), 1 μL 100× BSA (20 mg mL^{-1}) (NEB, B9000) and 400 ng pUC19 DNA were exposed to varying concentrations of each complex (0.01, 0.025, 0.05, 0.1, 0.5, 0.75, 1, 2.5, 7.5, 10, 20, 50, 100, 200, 400 μM) from HEPES stock for 30 min at room temperature. Subsequently 1 unit of *E. coli* topoisomerase I (NEB, M0301) was added and incubated for 15 min at 310 K. Reactions were quenched with SDS 0.25% and 250 μg mL^{-1} proteinase K (both from Sigma Aldrich, Ireland). Proteins were denatured with 30 min incubation at 323 K. 6× loading dye (Fermentas) was added to samples and loaded onto 1.2% agarose gel and subjected to gel electrophoresis at 40 V for 4 h and 50 V for 3.5 h in 1× TBE buffer at room temperature. The gel was post stained with 25 μM EtBr bath for 10 min and soaked for 24 h in deionised water.

4.7. *In vitro* anti-bacterial activity

In vitro anti-bacterial activity of test compounds were evaluated on a panel of three ATCC strains (*Staphylococcus aureus* (SA) ATCC 6538, *Escherichia coli* (EC) ATCC 8739, *Pseudomonas aeruginosa* (PA) ATCC 9027) and five clinical isolates (methicillin resistant *Staphylococcus aureus* (MRSA) HK5996/08, *Staphylococcus epidermidis* (SE) HK6966/08, *Enterococcus* sp. (EF) HK14365/08, *Klebsiella pneumonia* (KP) HK11750/08, *Klebsiella pneumoniae* ESBL (KPE) HK14368/08) from the collection of bacterial strains deposited at the Department of Biological and Medical Sciences, Faculty of Pharmacy, Charles University, Hradec Králové, Czech Republic. The above-mentioned ATCC strains also served as the quality control strains. All the isolates were maintained on Mueller-Hinton (MH) agar prior to being tested.

Minimum inhibitory concentrations (MICs) were determined by a modified Clinical and Laboratory Standards Institute (CLSI) standard of microdilution format of the M07-A7 document.[44] DMSO (100%) served as a diluent for all compounds; the final concentration did not exceed 2%. MH agar (HiMedia, Cadersky-Envitek, Czech Republic) buffered to pH 7.4 (±0.2) was used as the test medium. The wells of the microdilution tray contained 200 μL of the MH medium with 2-fold serial dilutions of the compounds (1000–0.244 μmol L^{-1}) and 10 μL of inoculum suspension. Inoculum in MH medium was prepared to give a final concentration of 0.5 McFarland scale (1.5×10^8 CFU mL^{-1}). The trays were incubated at 310 K, and MICs were read visually after 24 and 48 h. The MICs were defined as 95% inhibition of the control growth. MICs were determined twice and in duplicate. The deviations from the usually obtained values were no higher than the nearest concentration value up and down the dilution scale.

4.8. *In vitro* anti-fungal activity

In vitro anti-fungal activity of the compounds were evaluated on a panel of three ATCC strains (*Candida albicans* ATCC 44859 (CA1); *Candida albicans* ATCC 90028 (CA2); *Candida krusei* ATCC 6258 (CK1)) and eight clinical yeast isolates (*Candida krusei* E28 (CK2); *Candida tropicalis* 156 (CT); *Candida glabrata* 20/I (CG); *Candida lusitaniae* 2446/I (CL); *Trichosporon asahii* 1188 (TA)) and filamentous fungi (*Aspergillus fumigatus* 231 (AF); *Absidia corymbifera* 272 (AC); *Trichophyton mentagrophytes* 445 (TM)) from the collection of fungal strains deposited at the Department of Biological and Medical Sciences, Faculty of Pharmacy, Charles University, Hradec Králové, Czech Republic. Three ATCC strains were used as the quality control strains. All of the isolates were maintained on Sabouraud dextrose agar prior to being tested.

Minimum inhibitory concentrations (MICs) were determined by modified CLSI standard of microdilution format of the M27-A3 and M38-A2 documents.[35] DMSO (100%) served as a diluent for all compounds; the final concentration did not exceed 2%. RPMI-1640 (Sevapharma, Prague) medium supplemented with L-glutamine and buffered with 0.165 M morpholinepropanesulfonic acid (Serva) to pH 7.0 by 10 M NaOH was used as the test medium. The wells of the microdilution tray contained 200 μL of the RPMI-1640 medium with 2-fold serial dilutions of the compounds (1000–0.244 μmol L^{-1} for the new compounds) and 10 μL of inoculum suspension.

Fungal inoculum in RPMI-1640 was prepared to give a final concentration of $5 \times 10^3 \pm 0.2$ CFU mL^{-1}. The trays were incubated at 308 K, and MICs were read visually after 24 and 48 h. The MIC values for the dermatophytic strain (*T. mentagrophytes*) were determined after 72 and 120 h. The MICs were defined as 80% inhibition (IC_{80}) of the control growth for yeasts and as 50% inhibition (IC_{50}) of the control growth for filamentous fungi. MICs were determined twice and in duplicate. The deviations from the usually obtained values were no higher than the nearest concentration value up and down the dilution scale.

Abbreviations

AC	*Absidia corymbifera* 272
AF	*Aspergillus fumigatus* 231
bp	Base pair
CA1	*Candida albicans* ATCC 44859
CA2	*Candida albicans* ATCC 90028
CFU	Colony-forming unit
CG	*Candida glabrata* 20/I
Cip	Ciprofloxacin
CipA	Ciprofloxacin analogue *i.e.* 7-(4-(decanoyl) piperazin-1-yl) derivative of Cip
$CipA_{-H}$	Deprotonated ciprofloxacin analogue
CK1	*Candida krusei* ATCC 6258
CK2	*Candida krusei* E28
CL	*Candida lusitaniae* 2446/I
CP	*Candida parapsilosis* ATCC 22019
CT	*Candida tropicalis* 156
ctDNA	Calf thymus DNA
DMF	*N*,*N*-Dimethylformamide
DMSO	Dimethyl sulfoxide
DNA	Deoxyribonucleic acid
DPPN	Benzo[*i*]dipyridophenazine/benzo[*i*]dipyrido [3,2-*a*:2′,3′-*c*]phenazine
DPPZ	Dipyridophenazine/dipyrido[3,2-*a*:2′,3′-*c*] phenazine
DPQ	Dipyridoquinoxaline/dipyrido[3,2-*f*:2′,3′-*h*] quinoxaline
dsDNA	Double strand DNA
E. coli	Escherichia coli
EC	*Escherichia coli*
EF	*Enterococcus* sp.
eq	Equivalent
ESI-MS	Electrospray ionisation mass spectrometry
EtBr	Ethidium bromide
G. mellonella	*Galleria mellonella*
HEPES	2-[4-(2-Hydroxyethyl)piperazin-1-yl]ethane-sulfonic acid
Hpr-norf	*N*-Propyl protected form of norfloxacin
IR	Infra-red
J	Coupling constant
K. pneumoniae	*Klebsiella pneumoniae*
KP	*Klebsiella pneumoniae*
KP-E	*Klebsiella pneumoniae* ESBL positive
m/*z*	Mass to charge ratio
MH	Mueller-Hinton
MIC	Minimum inhibitory concentration
Moxi	Moxifloxacin
MRSA	Methicillin resistant *Staphylococcus aureus*
MTT	3-(4,5-Dimethylthiazol-2-yl)-2,5-diphenyltetrazolium bromide
P. aeruginosa	*Pseudomonas aeruginosa*
PA	*Pseudomonas aeruginosa*
PBS	Phosphate-buffer saline
phen	1,10-Phenanthroline/phenanthroline
phendione	1,10-Phenanthroline-5,6-dione
ROS	Reactive oxygen species
RPMI-1640	Roswell Park Memorial Institute medium
S. aureus	*Staphylococcus aureus*
SA	*Staphylococcus aureus*
SE	*Staphylococcus epidermidis*
stDNA	salmon testes DNA
TA	*Trichosporon asahii* 1188
TAE	Tris-Acetate-EDTA buffer
TBE	Tris-Borate-EDTA buffer
TH_2	Tiron/4,5-dihydroxy-1,3-benzenedisulfonic acid disodium salt
TM	*Trichophyton mentagrophytes* 445

Conflicts of interest

There are no conflicts to declare.

Acknowledgements

This material is based upon works supported by the Science Foundation Ireland under Grant No. [11/RFP.1/CHS/3095] and [17/TIDA/5009] and by RCSI. This work has also been funded under the Programme for Research in Third-Level Institutions and cofounded under the European Regional Development fund (BioAT programme). NG acknowledges funding from the European Union's Seventh Framework Programme for Research, Technological Development, and Demonstration under Grant Agreement No. 621364 (TUTIC-Green). CJM would also like to acknowledge COST CM1105 and COST CA15135 for being a platform to progress fruitful collaborations. A. K. also acknowledges funding from Science Foundation Ireland [15/CDA/3648] and the Marie Skłodowska-Curie Innovative Training Network (ITN) ClickGene (H2020-MSCA-ITN2014-642023).

References

1 (*a*) T. C. Johnstone, K. Suntharalingam and S. J. Lippard, *Chem. Rev.*, 2016, **116**, 3436–3486; (*b*) R. G. Kenny, S. W. Chuah, A. Crawford and C. J. Marmion, *Eur. J. Inorg.*

Chem., 2017, **2017**, 1596–1612; (*c*) R. G. Kenny and C. J. Marmion, *Chem. Rev.*, 2019, **119**, 1058–1137.
2 J. P. Parker, Z. Ude and C. J. Marmion, *Metallomics*, 2016, **8**, 43–60.
3 (*a*) T. McGivern, S. Afsharpour and C. J. Marmion, *Inorg. Chim. Acta*, 2018, **472**, 12–39; (*b*) C. Santini, M. Pellei, V. Gandin, M. Porchia, F. Tisato and C. Marzano, *Chem. Rev.*, 2014, **114**, 815–862; (*c*) A. Prisecaru, V. McKee, O. Howe, G. Rochford, M. McCann, J. Colleran, M. Pour, N. Barron, N. Gathergood and A. Kellett, *J. Med. Chem.*, 2013, **56**, 8599–8615.
4 N. T. Nassar, in *Element Recovery and Sustainability*, ed. A. Hunt, The Royal Society of Chemistry, Cambridge, 2013.
5 (*a*) F. Mancin, P. Scrimin and P. Tecilla, *Chem. Commun.*, 2012, **48**, 5545–5559; (*b*) Z. Yu and J. A. Cowan, *Curr. Opin. Chem. Biol.*, 2018, **43**, 37–42.
6 (*a*) L. Li, K. Du, Y. Wang, H. Jia, X. Hou, H. Chao and L. Ji, *Dalton Trans.*, 2013, **42**, 11576–11588; (*b*) A. Kellett, M. O'Connor, M. McCann, M. McNamara, P. Lynch, G. Rosair, V. McKee, B. Creaven, M. Walsh, S. McClean, A. Foltyn, D. O'Shea, O. Howe and M. Devereux, *Dalton Trans.*, 2011, **40**, 1024–1027; (*c*) K. Li, L. H. Zhou, J. Zhang, S. Y. Chen, Z. W. Zhang, J. J. Zhang, H. H. Lin and X. Q. Yu, *Eur. J. Med. Chem.*, 2009, **44**, 1768–1772; (*d*) S. S. Tonde, A. S. Kumbhar, S. B. Padhye and R. J. Butcher, *J. Inorg. Biochem.*, 2006, **100**, 51–57.
7 D. S. Sigman, D. R. Graham, V. D'Aurora and A. M. Stern, *J. Biol. Chem.*, 1979, **254**, 12269–12272.
8 Z. Molphy, A. Prisecaru, C. Slator, N. Barron, M. McCann, J. Colleran, D. Chandran, N. Gathergood and A. Kellett, *Inorg. Chem.*, 2014, **53**, 5392–5404.
9 (*a*) T. J. P. McGivern, C. Slator, A. Kellett and C. J. Marmion, *Mol. Pharm.*, 2018, **15**, 5058–5071; (*b*) C. Slator, Z. Molphy, V. McKee, C. Long, T. Brown and A. Kellett, *Nucleic Acids Res.*, 2018, **46**, 2733–2750; (*c*) Z. Molphy, D. Montagner, S. S. Bhat, C. Slator, C. Long, A. Erxleben and A. Kellett, *Nucleic Acids Res.*, 2018, **46**, 2733–2750.
10 M. B. Lustberg, *Clin. Adv. Hematol. Oncol.*, 2012, **10**, 825–826.
11 V. A. Morrison, *Supportive Cancer Ther.*, 2005, **2**, 88–94.
12 L. B. Norris, F. Kablaoui, M. K. Brilhart and P. B. Bookstaver, *Int. J. Antimicrob. Agents*, 2017, **50**, 308–317.
13 S. Celebi, M. E. Sezgin, D. Cakir, B. Baytan, M. Demirkaya, B. Sevinir, S. E. Bozdemir, A. M. Gunes and M. Hacimustafaoglu, *Pediatr. Hematol. Oncol.*, 2013, **30**, 187–194.
14 M. P. Veve, S. L. Davis, A. M. Williams, J. E. McKinnon and T. A. Ghanem, *Oral Oncol.*, 2017, **74**, 181–187.
15 J. C. Cho, M. P. Crotty, B. P. White and M. V. Worley, *Pharmacotherapy*, 2018, **38**, 108–121.
16 R. Singh, R. N. Jadeja, M. C. Thounaojam, R. V. Devkar and D. Chakraborty, *Transition Met. Chem.*, 2012, **37**, 541–551.
17 E. K. Efthimiadou, H. Thomadaki, Y. Sanakis, C. P. Raptopoulou, N. Katsaros, A. Scorilas, A. Karaliota and G. Psomas, *J. Inorg. Biochem.*, 2007, **101**, 64–73.
18 https://www.who.int/medicines/publications/essentialmedicines/en/(accessed 22/10/2018).
19 N. Jimenez-Garrido, L. Perello, R. Ortiz, G. Alzuet, M. Gonzalez-Alvarez, E. Canton, M. Liu-Gonzalez, S. Garcia-Granda and M. Perez-Priede, *J. Inorg. Biochem.*, 2005, **99**, 677–689.
20 P. Drevensek, I. Leban, I. Turel, G. Giester and E. Tillmanns, *Acta Crystallogr., Sect. C: Cryst. Struct. Commun.*, 2003, **59**, m376–m378.
21 J. Azema, B. Guidetti, A. Korolyov, R. Kiss, C. Roques, P. Constant, M. Daffe and M. Malet-Martino, *Eur. J. Med. Chem.*, 2011, **46**, 6025–6038.
22 Z. Ude, I. Romero-Canelon, B. Twamley, D. Fitzgerald Hughes, P. J. Sadler and C. J. Marmion, *J. Inorg. Biochem.*, 2016, **160**, 210–217.
23 (*a*) M. Vincent, R. E. Duval, P. Hartemann and M. Engels-Deutsch, *J. Appl. Microbiol.*, 2018, **124**, 1032–1046 and references therein; (*b*) G. Borkow and J. Gabbay, *Curr. Med. Chem.*, 2005, **12**, 2163–2175.
24 A. G. Orpen, L. Brammer, F. H. Allen, O. Kennard, D. G. Watson and R. Taylor, *Dalton Trans.*, 1989, S1–S83.
25 G. Mendoza-Díaz, L. M. R. Martinez-Aguilera, R. Perez-Alonso, X. Solans and R. Moreno-Esparza, *Inorg. Chim. Acta*, 1987, **138**, 41–47.
26 K. Nakamoto, *Infrared and Raman Spectra of Inorganic and Coordination Compounds*, John Wiley & Sons, Inc., New Jersey, 6th edn, 2009.
27 T. Mosmann, *J. Immunol. Methods*, 1983, **65**, 55–63.
28 https://www.cancer.gov/about-cancer/understanding/statistics (accessed 22/10/2018).
29 M. O'Connor, A. Kellett, M. McCann, G. Rosair, M. McNamara, O. Howe, B. S. Creaven, S. McClean, A. F. Kia, D. O'Shea and M. Devereux, *J. Med. Chem.*, 2012, **55**, 1957–1968.
30 C. Liu, Y. Zhu, W. Lou, N. Nadiminty, X. Chen, Q. Zhou, X. B. Shi, R. W. deVere White and A. C. Gao, *Prostate*, 2013, **73**, 418–427.
31 K. Suzuki and H. Matsubara, *J. Biomed. Biotechnol.*, 2011, **2011**, 978312.
32 A. Petitjean, M. I. Achatz, A. L. Borresen-Dale, P. Hainaut and M. Olivier, *Oncogene*, 2007, **26**, 2157–2165.
33 B. Pang, X. Qiao, L. Janssen, A. Velds, T. Groothuis, R. Kerkhoven, M. Nieuwland, H. Ovaa, S. Rottenberg, O. van Tellingen, J. Janssen, P. Huijgens, W. Zwart and J. Neefjes, *Nat. Commun.*, 2013, **4**, 1908.
34 M. McCann, J. McGinley, K. Ni, M. O'Connor, K. Kavanagh, V. McKee, J. Colleran, M. Devereux, N. Gathergood, N. Barron, A. Prisecaru and A. Kellett, *Chem. Commun.*, 2013, **49**, 2341–2343.
35 (*a*) C. Bailly, N. Pommery, R. Houssin and J. P. Henichart, *J. Pharm. Sci.*, 1989, **78**, 910–917; (*b*) A. Kellett, M. O'Connor, M. McCann, O. Howe, A. Casey, P. McCarron, K. Kavanagh, M. McNamara, S. Kennedy, D. D. May, P. S. Skell, D. O'Shea and M. Devereux, *MedChemComm*, 2011, **2**, 579–584; (*c*) A. W. McConnaughie and T. C. Jenkins, *J. Med. Chem.*, 1995, **38**, 3488–3501.

36 J. J. Champoux, *Annu. Rev. Biochem.*, 2001, **70**, 369–413.
37 K. N. Kreuzer and N. R. Cozzarelli, *J. Bacteriol.*, 1979, **140**, 424–435.
38 K. J. Aldred, H. A. Schwanz, G. Li, B. H. Williamson, S. A. McPherson, C. L. Turnbough, Jr., R. J. Kerns and N. Osheroff, *Biochem.*, 2015, **54**, 1278–1286.
39 A. Naeem, S. L. Badshah, M. Muska, N. Ahmad and K. Khan, *Molecules*, 2016, **21**, 268.
40 K. J. Aldred, H. A. Schwanz, G. Li, S. A. McPherson, C. L. Turnbough, Jr., R. J. Kerns and N. Osheroff, *ACS Chem. Biol.*, 2013, **8**, 2660–2668.
41 W. Zhou, X. Wang, M. Hu, C. Zhu and Z. Guo, *Chem. Sci.*, 2014, **5**, 2761–2770.
42 L. M. Assis, M. Nedeljkovic and A. Dessen, *Drug Resist. Updates*, 2017, **31**, 1–14.
43 https://www.who.int/medicines/areas/rational_use/antibacterial_agents_clinical_development/en/ (accessed 22/10/2018).
44 (*a*) B. Albada and N. Metzler-Nolte, *Acc. Chem. Res.*, 2017, **50**, 2510–2518; (*b*) M. Patra, M. Wenzel, P. Prochnow, V. Pierroz, G. Gasser, J. E. Bandow and N. Metzler-Nolte, *Chem. Sci.*, 2015, **6**, 214–224; (*c*) M. Wenzel, M. Patra, C. H. Senges, I. Ott, J. J. Stepanek, A. Pinto, P. Prochnow, C. Vuong, S. Langklotz, N. Metzler-Nolte and J. E. Bandow, *ACS Chem. Biol.*, 2013, **8**, 1442–1450.
45 K. Kavanagh and E. P. Reeves, *FEMS Microbiol. Rev.*, 2004, **28**, 101–112.
46 J. C. Junqueira, *Virulence*, 2012, **3**, 474–476.
47 N. Dolan, D. P. Gavin, A. Eshwika, K. Kavanagh, J. McGinley and J. C. Stephens, *Bioorg. Med. Chem. Lett.*, 2016, **26**, 630–635.
48 (*a*) C. J. Tsai, J. M. Loh and T. Proft, *Virulence*, 2016, **7**, 214–229; (*b*) S. M. Cook and J. D. McArthur, *Virulence*, 2013, **4**, 350–353; (*c*) M. Brennan, D. Y. Thomas, M. Whiteway and K. Kavanagh, *FEMS Immunol. Med. Microbiol.*, 2002, **34**, 153–157.
49 R. Maguire, M. Kunc, P. Hyrsl and K. Kavanagh, *Comp. Biochem. Physiol., Part C: Toxicol. Pharmacol.*, 2017, **195**, 44–51.
50 M. McCann, A. L. S. Santos, B. A. da Silva, M. T. V. Romanos, A. S. Pyrrho, M. Devereux, K. Kavanagh, I. Fichtner and A. Kellett, *Toxicol. Res.*, 2012, **1**, 47–54.
51 G. Sheldrick, *Acta Crystallogr., Sect. A: Found. Adv.*, 2015, **71**, 3–8.
52 G. Sheldrick, *ta Crystallogr., Sect. A: Found. Crystallogr.*, 2008, **64**, 112–122.
53 O. V. Dolomanov, L. J. Bourhis, R. J. Gildea, J. A. K. Howard and H. Puschmann, *J. Appl. Crystallogr.*, 2009, **42**, 339–341.
54 N. Browne, F. Hackenberg, W. Streciwilk, M. Tacke and K. Kavanagh, *Biometals*, 2014, **27**, 745–752.
55 P. Peixoto, C. Bailly and M.-H. David-Cordonnier, Topoisomerase I-Mediated DNA Relaxation as a Tool to Study Intercalation of Small Molecules into Supercoiled DNA, in *Drug-DNA Interaction Protocols*, ed. K. Fox, Humana Press, New Jersey, USA, 2nd edn, 2010, vol. 613, pp. 235–256.